

The Visualization of Two-Dimensional Second-Order Tensor Fields

Burkhard Wünsche

Department of Computer Science, The University of Auckland
Private Bag 92019, Auckland, New Zealand
Email: burkhard@cs.auckland.ac.nz

Abstract: This paper gives an introduction to the visualization of two-dimensional second-order tensor fields. We present an extended classification framework for tensor field icons, suggest several small improvements, and demonstrate the usefulness of the implemented methods on a real-world example.

Keywords: Scientific visualization, tensor fields, stress fields

1 Introduction

Second-order tensors are a fundamental entity in engineering, physical sciences and biomedicine. Examples are stresses and strains in solids and viscous stresses and velocity gradients in fluid flows. It can also be shown that tensor data correlates large amount of non-tensor quantities such as pressure, kinetic energy density, and mass density [3].

Unfortunately second-order tensors have the same complexity as matrices. Large amounts of tensor data are hence difficult to interpret. Nonetheless the visualization of tensor fields improves the understanding and interpretation of tensor data and is therefore of paramount importance for the scientist.

In this paper we introduce an extended framework to classify tensor field visualization methods and suggests several improvements for existing visualization methods.

2 Notations, Definitions, and Examples

For simplicity we use a rectangular Cartesian coordinate system with the base vectors \mathbf{e}_1 , \mathbf{e}_2 , and \mathbf{e}_3 . Vectors are written in small bold Latin letters and tensors in capital bold Latin letters or small bold Greek letters.

A second-order tensor can be understood as a linear transformation between two vectors and can be represented by a matrix. An example is the *stress tensor* which describes the external forces acting throughout a solid body and is important when examining and predicting material failure.

To define the stress tensor consider the external forces acting on a real or imagined surface within the body. The surface force at a point of the surface is described by a *stress vector*. Consider a plane S with normal \mathbf{n} at a point P of the elastic body as shown in figure 1. Let $\Delta\mathbf{f}$ be the force acting on a small area ΔA containing P . The stress vector \mathbf{t}_n at P is defined as

$$\mathbf{t}_n = \lim_{\Delta A \rightarrow 0} \frac{\Delta\mathbf{f}}{\Delta A}$$

In classical continuum theory the resulting stress vector is the same for all surfaces through point P with a tangent plane S in P , i.e., it is independent of the surface curvature. It can be shown ([8]) that the stress vector acting on any plane with normal \mathbf{n} through P can be expressed as

$$\mathbf{t}_n = \boldsymbol{\sigma} \mathbf{n}$$

where the linear operator $\boldsymbol{\sigma}$ defines the *stress tensor* in P .

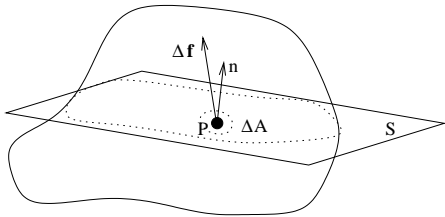


Figure 1: Definition of a stress vector.

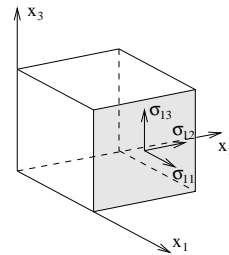


Figure 2: Stress components of a tensor.

To interpret the components of the stress tensor $\boldsymbol{\sigma}$ consider an infinitesimal small axis-aligned cube as shown in figure 2. The stress tensor components σ_{11} , σ_{12} , and σ_{13} are the components of the stress vector $\mathbf{t}_{\mathbf{e}_1}$. The other components of $\boldsymbol{\sigma}$ are interpreted similarly. We call the diagonal elements σ_{11} , σ_{22} , and σ_{33} the *normal stresses* and the off-diagonal elements σ_{12} , σ_{13} , σ_{23} , σ_{21} , σ_{31} , and σ_{32} the *shear stresses*. By using the conservation of momentum equation it can be shown that $\boldsymbol{\sigma}$ is symmetric for most materials [5].

An important property of any n -dimensional symmetric tensor \mathbf{T} is that there always exist n *eigenvalues* λ_i and n mutually perpendicular *eigenvectors* \mathbf{v}_i such that

$$\mathbf{T}\mathbf{v}_i = \lambda_i\mathbf{v}_i \quad i = 1, \dots, n \quad (1)$$

The eigenvalues of a stress tensor $\boldsymbol{\sigma}$ are usually called the *principal stresses* and the corresponding eigenvectors are called *principal directions*.

3 Visualization of Tensor fields

The difficulty of interpreting tensor data arises not only from the usually large size of the data sets but also from the fact that each tensor is represented by a matrix. The aim of tensor field visualization is therefore to transform these large amount of data into a single image which can be easily understood and interpreted by the user.

Two useful tools in visualizing data are *data transformation* and *data reduction*. Data transformation retains all the information in the data but presents it in a different form. We have already presented the transformation of a tensor into its eigenvectors and eigenvalues. In 2D the tensor field is then represented by two orthogonal vector fields and two scalar fields. Another popular transformation is given by a change of coordinate systems.

Data reduction on the other hand extracts only partial information from the original tensor data and so gives an incomplete representation. We distinguish by the type of the reduced data, e.g., vector or scalar. Examples of *vector data* obtained by reducing tensor data are the eigenvectors of a tensor \mathbf{T} and the *surface reaction vector* obtained by multiplying the tensor with the surface normal.

Scalar data obtained by reducing tensor data includes the eigenvalues and directions of the eigenvectors (e.g., given by its angle with the x_1 -axis).

3.1 Classification of Tensor Icons

Having determined what form of data transformation or reduction is appropriate for a given tensor field, the problem is now to visualize the selected data. The visualization is by means of geometric objects with visual attributes, so-called *tensor icons*. We first present a classification of tensor icons before giving a more detailed explanation.

Our classification is a modification and extension of a framework originally introduced in [6]. Tensor icons are classified according to the covered *spatial domain* and the embodied *information level*, which we call the *information scope*. We additionally classify by the inherent *information type*. As a result we get a three-dimensional classification matrix as shown in table 1.

Info. Type	Spatial Domain	Information Scope		
		Elementary	Local	Global
Tensor	Point	tensor ellipsoid, tensor cross, tensor glyph	degenerate point	topology
	Line	hyperstreamline		
	Surface			
Vector	Point	tensor line		
	Line	tensor streamline		
	Surface	spot noise		
Scalar	Point			
	Line			isocontours
	Surface	colour mapping, height field		

Table 1: Tensor icons containing full tensor information, vector information, and scalar information.

In two dimensions the *spatial domain* is either a point, a line, or a surface. The embodied *information scope* is *elementary* if the icon represents the data only across the extent of its spatial domain; *local* if in addition derivative information (e.g., gradient, curl) is displayed; and *global* if the icon represents the structure of the whole tensor field. The *information type* gives the type of information displayed after data reduction, in our case scalar, vector, or tensor.

We explain and demonstrate the effectiveness of tensor icons with the help of a real-world example. Figure 3 (a) shows a plate with a hole under uniaxial load. Because of symmetry we model only one quarter of the original plate. To compute the resulting deformation and stresses and strains in the plate we implemented a *Finite Element Method* modeller.

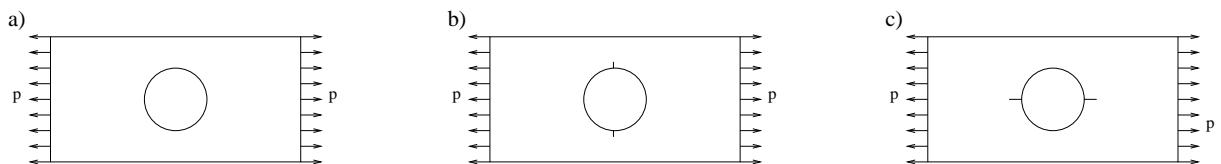


Figure 3: Plate with a hole without (a) and with (b,c) cracks.

3.2 Tensor Icons Containing Scalar Information

2D scalar data can be visualized by mapping the data into a colour spectrum. For example consider figure 4 which shows the plate from figure 3 (a) in green solid lines and the deformed plate in dashed lines. Since the deformations are very small the displacement field has been scaled. The maximum principal stress is visualized by colour mapping. The colour spectrum used interpolates linearly between white-yellow, saturated yellow, saturated red, saturated blue and blue-black. It is clearly visible that the maximum principal tensile stress occurs at the top of the hole which is therefore the area where the material is most likely to fail. Note that the linear colour map used makes it very difficult to differentiate stress values and stress contours at the bottom half of the plate. An improvement is achieved in figure 5 by defining a cyclical colour map and mapping the scalar data over eight colour cycles.

Another technique is to interpret 2D scalar data as a *height field*. A second scalar field can then be colour mapped onto the surface of the height field which is useful when looking for relationships between two scalars derived from the same or different tensors.

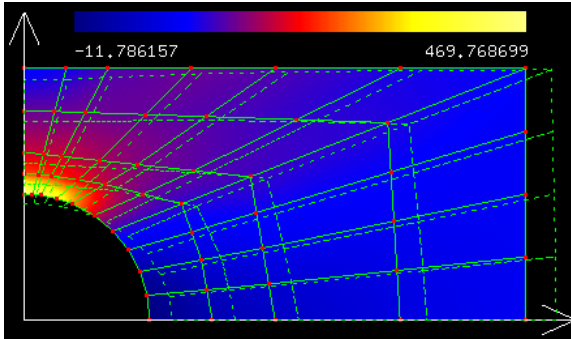


Figure 4: Maximum principal stress visualized by colour mapping.

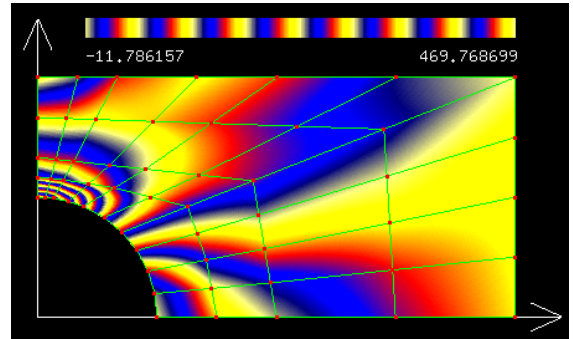


Figure 5: Maximum principal stress visualized using a cyclical colour map.

The c -*isocontour* of a scalar field s is defined as all points \mathbf{x} for which $s(\mathbf{x}) = c$. In contrast to a colour mapped scalar field isocontours occupy only a small area of the image and can therefore be easily combined with other visualization icons. Figure 8 shows the isocontours of the maximum principal stress in combination with tensor ellipsoids which give additionally the principal directions of the stress tensor (see subsection 3.4).

3.3 Tensor Icons Containing Vector Information

The eigenvector of a tensor at a point can be visualized by a simple line segment created at that point. The direction and length of this *tensor line* is given by the eigenvector and the corresponding eigenvalue, respectively. Note that the line can not be replaced by an arrow since with equation 1 the signs of the eigenvectors are indeterminate. The same icon can be used for other derived vector data with indeterminate sign, such as the direction of the maximum shear stress.

The obvious disadvantage of using tensor icons at discrete points is that using too few might fail to reveal interesting areas of the tensor field, but using too many leads to visual cluttering which makes interpretation difficult. A continuous representation of a vector field \mathbf{v} derived from a tensor is achieved by a *tensor streamline* which is an integral curve $\mathbf{x}(s)$ satisfying

$$\frac{d\mathbf{x}}{ds} = \mathbf{v}(\mathbf{x}) \quad (2)$$

The tensor streamline is colour coded with an appropriate scalar field: for example, if using an eigenvector field we would use the corresponding eigenvalue field as shown in figure 6. Because eigenvectors have indeterminate sign the tensor streamline is always traced in both the positive and negative directions. This is not the case if using streamlines in traditional vector field visualization (e.g., for fluid flow).

One problem with tensor streamlines is the difficulty in placing them. If they are too close together they merge and the directional information is obscured. If the tensor streamlines are too far apart, as in some areas of figure 6, information is missing for large areas. One solution is *spot noise*, shown in figure 7, which is generated by distorting a noise texture with the derived vector field [1].

3.4 Tensor Icons Containing Full Tensor Information

Tensor crosses are constructed by two lines, the directions and lengths of which are given by the eigenvectors and eigenvalues of the tensor, respectively. For a *tensor ellipsoid* the eigenvectors give the principal axis. Examples are given in figure 8 and figure 9. We additionally visualize the sign of each eigenvalue by using a dark colour for a negative value and a bright colour for a positive value. More sophisticated icons are given by Haber [4].

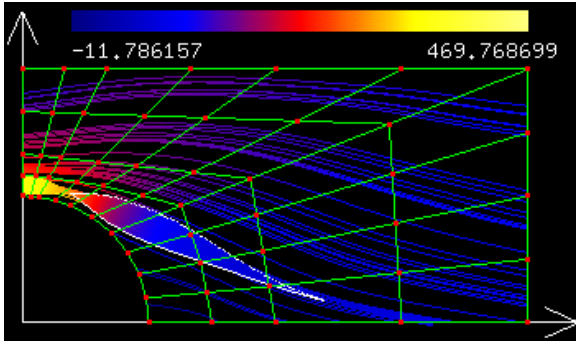


Figure 6: Maximum principal stress visualized with tensor field lines and one hyperstreamline.

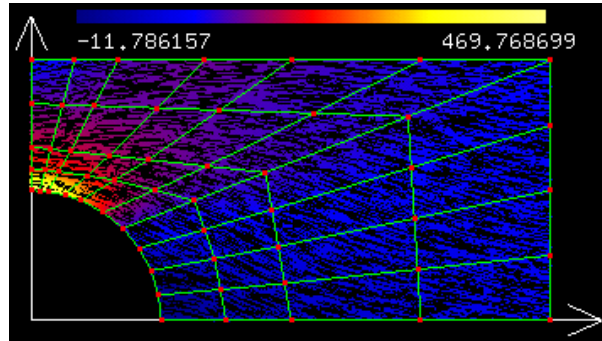


Figure 7: Maximum principal stress visualized by spot noise.

The importance of the direction of the principal stress is demonstrated by considering again the plate with a hole under uniaxial load in figure 3. In part (b) of the figure the plate has a crack in the top and bottom (for symmetry reasons) of the hole. In part (c) of the figure cracks are in the left and right hand side of the hole. The left part of figure 9 shows that under the applied load the crack at the top opens and the maximum principal stress increases at the tip of the crack. The added tensor crosses show that the maximum principal stress is a tensile stress approximately normal to the crack boundary. This means that once a crack develops at the top of the plate the plate is likely to rupture. In contrast the right-hand side of figure 9 shows that the stresses around the crack on the right-hand side of the hole are small and compressive perpendicular to the crack boundary (look for the two small lines in dark cyan). This means that the crack would close under the applied load.

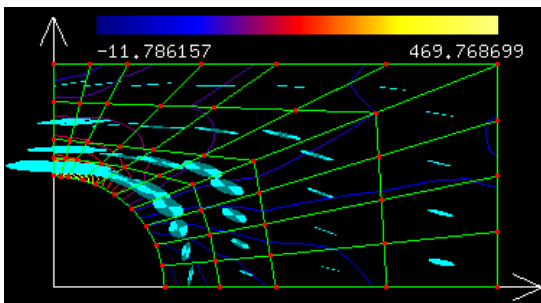


Figure 8: Stress field visualized by tensor ellipsoids and the isocontours of the maximum principal stress.

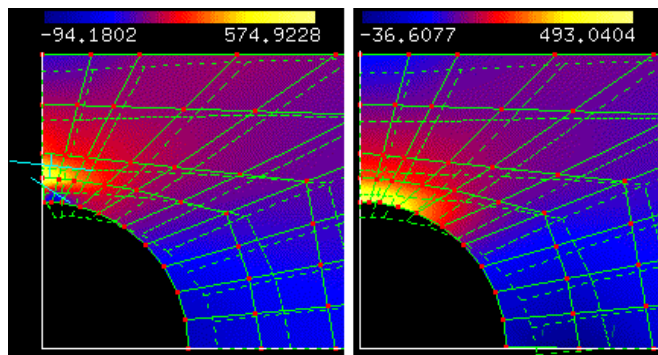


Figure 9: Maximum principal stress in a plate with (left image) crack at the top of the hole and (right image) crack at the bottom of the hole.

Too many tensor crosses or tensor ellipsoids placed densely together might lead to visual clutter. Perception is improved by using a *hyperstreamline* [6]. The trajectory of a hyperstreamline is a tensor streamline of an eigenvector field. The corresponding second eigenvector and eigenvalue define the diameter of the hyperstreamline at each point. A negative eigenvalue is indicated by adding a white boundary to the hyperstreamline. Figure 6 shows that the complete information about both the major and minor eigenvector fields along the trajectory is revealed.

Degenerate points are points for which two eigenvalues of the tensor are equal. It can be shown that in this case all vectors in a plane are eigenvectors. Degenerate points are therefore the only points where the trajectories of an eigenvector field can cross. Delmarcelle shows that the derivatives of the tensor components can be used to derive the direction in which *separatrices* emanate from the degenerate point [2]. The separatrices are trajectories of the major eigenvector field separating it into regions of similar behaviour and therefore define the *topology* of the tensor field. The stress field for a plane under uniaxial

load is too simple to contain any degenerate points. Hesselink and Delmarcelle give some examples for tensor field topology as they occur in fluid dynamics [7].

4 Conclusion

Interpreting large amounts of tensor data is difficult since a tensor is equivalent to a matrix. As a solution we have presented two techniques to extract useful information from a tensor, and we have given examples showing how tensor icons can be used to visualize that information.

We also introduced an extended classification framework for tensor icons. Several small improvements for existing tensor field visualization methods were suggested and the usefulness of the presented methods was demonstrated on an easily understandable real-world example.

References

- [1] Willem C. de Leeuw and Jarke J. van Wijk. Enhanced spot noise for vector field visualization. In Gregory M. Nielson and Deborah Silver, editors, *Proceedings of Visualization '95*, pages 233 – 239, Los Alamitos, California, 1995. IEEE, Computer Society Press.
- [2] Thierry Delmarcelle. *The Visualization of Second-Order Tensor Fields*. PhD thesis, Stanford University, 1994. URL: <http://www.nas.nasa.gov/NAS/TechReports/RelatedPapers/StanfordTensorFieldVis/DelmarcelleThesis/abstract.html>.
- [3] Thierry Delmarcelle and Lambertus Hesselink. Visualizing second order tensor fields with hyperstreamlines. *IEEE Computer Graphics and Applications*, 13(4):25 – 33, 1993.
- [4] R. B. Haber. Visualization techniques for engineering mechanics. *Computing Systems in Engineering*, 1(1):37 – 50, January 1990.
- [5] David Henwood and Javier Bonet. *Finite Elements - A Gentle Introduction*. MacMillian Press Ltd., 1996.
- [6] Lambertus Hesselink and Thierry Delmarcelle. Visualization of vector and tensor data sets. In L. J. Rosenblum et. al., editor, *Scientific Visualization: advances and challenges*, pages 419 – 433. Academic Press, London, 1994.
- [7] Lambertus Hesselink, Yuval Levy, and Yingmei Lavin. The topology of symmetric, second-order 3d tensor fields. *IEEE Transactions on Visualization and Computer Graphics*, 1997.
- [8] W. Michael Lai, David Rubin, and Erhard Krempl. *Introduction to Continuum Mechanics*, volume 17 of *Pergamon Unified Engineering Series*. Pergamon Press, Headington Hill Hall, Oxford OX3 0BW, England, revised SI/metric units edition, 1986.